


Dust-acoustic soliton breaking and the associated acceleration of charged particlesF. M. Trukhachev ^{1,2,3,*} M. M. Vasiliev,^{1,2} O. F. Petrov,^{1,2} and E. V. Vasilieva²¹*Moscow Institute of Physics and Technology, 141701 Dolgoprudny, Moscow Region, Russian Federation*²*Joint Institute for High Temperatures of the Russian Academy of Sciences, 125412, Moscow, Russian Federation*³*Belarusian-Russian University, 212000 Mogilev, Republic of Belarus* (Received 20 May 2019; revised manuscript received 12 September 2019; published 3 December 2019)

The breaking of a plane self-excited dust-acoustic soliton in a dust cloud formed in stratified dc glow discharge plasma is studied. Both macroscopic and kinetic parameters of the dust component near the soliton are experimentally obtained. It is shown that the breaking of a soliton can accelerate charged particles to supersonic speeds. The theoretical interpretation of the experimental results is performed in the framework of the hydrodynamic plasma approach, as well as the single-particle approximation. Both dissipative and nondissipative cases are considered.

DOI: [10.1103/PhysRevE.100.063202](https://doi.org/10.1103/PhysRevE.100.063202)**I. INTRODUCTION**

A soliton is commonly referred to as a solitary nonlinear wave that exists due to the balance of nonlinearity and dispersion of the medium. Since their discovery [1], solitons have been found in many media (surface solitons in a liquid, solitons in a plasma, solitons in power transmission lines), and the main properties of solitons have been studied in detail (see, for example, [2]). Nowadays we can say that solitons are the fundamental elements of nonlinear wave physics. The theoretical description of solitons in a conservative system is carried out in the framework of the KdV equation, which has an exact, though tedious solution in the context of the inverse scattering problem [3]. To describe self-excited solitons in open dissipative systems, the concept of the “dissipative soliton” is used [4,5]. This concept considers solitons as an element of the self-organization process. To describe the strong dissipative soliton (under conditions of strong dissipation), the complex Ginzburg-Landau equation [6] is used. However, as shown in [7,8], under conditions of weak dissipation, plasma dissipative solitons have a classical profile that can be found using classical methods (for example, the reductive perturbation technique), because the main properties of the soliton are still determined by the nonlinearity and dispersion of the medium. In this case, nonconservative forces determine only the evolution of the wave.

In many practically important problems, for example, in plasma, analysis of solitons can be performed within the bounds of the stationary Poisson equation describing solitons that have passed through all stages of evolution and are moving in a homogeneous medium with a constant velocity. In plasma without a magnetic field there are three types of solitons which can be distinguished: ion-, electron-, and dust-acoustic ones [9–11]. All the indicated types of solitons can be described in terms of the hydrodynamic plasma models, and in the simplest one-dimensional case, it can be reduced

to the stationary Poisson equation. Practically all solitons turn out to be supersonic in the sense of the parent wave mode, i.e. $M = V/C_{e,i,d} > 1$, where M is the Mach number; V soliton velocity; C_e , C_i , C_d electron-, ion-, and dust-acoustic phase velocities, respectively.

The velocity of solitons increases with the growth of the amplitude of their potential, φ_0 . Amplitude growth is limited by the value of $\varphi_{0\max}$ at which multistreaming flow occurs. Let us consider this phenomenon using ion-acoustic solitons as an example: when $\varphi_0 > \varphi_{0\max}$, ions are accelerated by the leading edge of a soliton up to velocities exceeding V ; at this the arising ion flow reduces the soliton energy (this process was described in detail in [12]). Moreover, multistreaming flow is associated with the breaking of a soliton, since in this case the condition of equality of plasma parameters before and after the wave front is violated. It is worth noting a large number of theoretical works on the stability of solitons and their evolution [12–14], but there are very few detailed experimental studies on this topic [9]. Parameters of multistreaming flow are practically not investigated. At the same time, the process of strong electron plasma waves breaking has been studied both experimentally [15,16] and theoretically [17,18]. The excitation of the strong electron plasma waves is due to the energy of the electromagnetic wave (pump). In this case, the plasma wave is a wave packet containing many maximums and minimums (in contrast to the soliton). At high pump powers, caviton formation was observed [19], as well as wave breaking and energetic particle generation. This topic has many applications, such as fusion, x-ray generation, particle acceleration, ionospheric heating, etc. The wave-particle interaction was experimentally investigated in [20] in a rf discharge dusty plasma. Trajectories of individual particles were analyzed; the parameters of the particles in resonance with the wave packet were determined. However, wave breaking, as well as particle acceleration, have not been studied in detail. In [21], breaking of the self-excited nonlinear dust-acoustic wave was studied. The analysis of the results was carried out in the framework of the Lagrangian-Eulerian model based on the wave-particle interaction, which made it possible to

*ftru@mail.ru

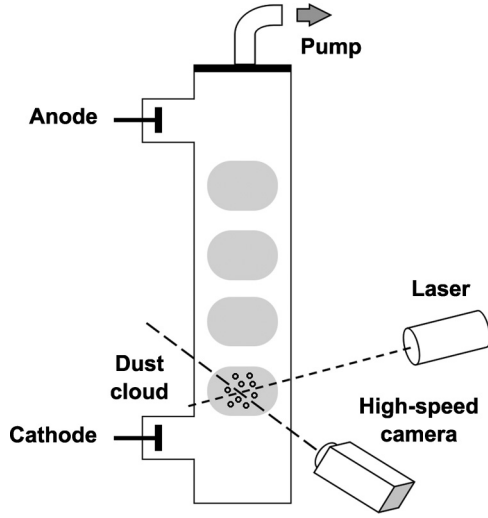


FIG. 1. Scheme of an experimental setup for studies of dusty plasma in dc low-temperature glow discharge.

estimate the wavelength and also to explain the breaking process by the intersection of neighboring particle trajectories. However, a detailed analysis of multistreaming flow was not performed. In addition, in [20,21] there are no models of dust-acoustic waves (both linear and nonlinear). It is worth noting works [22–24], where the acceleration and transfer of charged particles are theoretically and experimentally studied in the electric fields of solitons. It is shown that solitons can accelerate cold populations of particles to the velocities much higher than their thermal velocities, and the current excited in this case has a pulsed structure with a large dc component. In [24], the evolution of solitons has been analyzed until the moment of breaking, but the question of what happens to the kinetic energy of the particles after that still remains unsolved. These arguments determine the fundamental significance of research in this area. The applied significance of the work is related to the relevance of the problem of charged particle acceleration in plasma (see, for example [25]). On the other hand, solitons play an important role in the study of plasma turbulence [26] and in relevant applications, including nuclear fusion, star physics, etc.

In the present article, the breaking of a self-excited dust-acoustic soliton in a dust cloud in a low-pressure glow discharge is studied in detail. The main focus is on the analysis of multistreaming flow as well as on the acceleration of charged particles by a wave with supercritical amplitude. The preference of dusty plasma as an object of research is determined by the relative ease in conducting experimental studies at the kinetic level using simple optical devices. The theoretical interpretation of the experimental results is carried out in the framework of the hydrodynamic model of plasma and the single-particle approximation.

II. EXPERIMENTAL SETUP

The studies were carried out in a low-pressure dc glow discharge formed in a vertical tube 80 cm in height and 4 cm in diameter. The scheme of the experimental setup is shown in Fig. 1. Neon was used as a buffer gas, the pressure of which

TABLE I. Basic parameters of the plasma.

Buffer gas pressure	$P_{Ne} = 0.11$ Torr
Discharge current	$I = 0.6$ mA
Discharge voltage	$U = 1.27$ kV
Concentration of neutral atoms (buffer gas)	$n_a = 3.5 \times 10^{15}$ cm $^{-3}$
Concentration of electrons	$n_e = 1.5 \times 10^8$ cm $^{-3}$
Concentration of ions	$n_i = 4.5 \times 10^8$ cm $^{-3}$
Concentration of dust particles	$n_{0d} = 3.7 \times 10^4$ cm $^{-3}$
Framing rate	$f = 500$ fps
Pixel size	$h = 12.7$ μ m
Buffer gas temperature (discharge tube walls)	$T_a \approx 300$ K (0.03 eV)
Electron temperature (see [28,31])	$T_e \approx 6 \times 10^4$ K (6 eV)
Ion temperature (see [32,33])	$T_i \sim 1000$ K (0.1 eV)
Screening radius	$\lambda_D \approx \lambda_{Di} = 100$ μ m
Plasma frequency for the dust component	$\omega_d = 327$ s $^{-1}$
Dust-acoustic velocity	$C_d = 3.4$ cm/s
Dust particle mass	$m_d = 6.4 \times 10^{-11}$ g
Dust particle charge	$Z = 8 \times 10^3$ e
Interparticle distance	$L \approx 300$ μ m
Electric field	$E \sim 5$ V/cm
Reduced electric field	$E/N \sim 100$ Td

varied in the range of 0.08–0.125 Torr at a current of 0.6 mA. To provide a uniformity of parameters of the pressure and composition of the buffer gas, the discharge tube was continuously pumped out and filled with high-purity neon under monitoring of a pressure controller. Melamine formaldehyde particles with a diameter of $d_p = 4.25 \pm 0.09$ μ m were used as the dust component. Particles were injected into discharge from a container located at the upper part of the discharge tube. In glow discharge they gained an electric charge and formed dust clouds levitating at each striation due to being confined by an electrostatic trap. Experimental observations were performed at the lowest striation which was illuminated by means of a solid-state laser with wavelength 532 nm and power 0.1 W. The width of the laser “knife” was ~ 200 μ m. Parameters of the experiment as well as discharge parameters are presented in Table I. Dust density n_{0d} was obtained from video analysis. The typical magnitude of electron density in dc glow discharges is on the order of $n_e \sim 10^{-8} - 10^{-9}$ cm $^{-3}$ [11,27,28]. For calculations, we took the value $n_e = 1.5 \times 10^{-8}$ cm $^{-3}$ from [28], where discharge dusty plasma with close parameters was studied. Ion density is found from the quasineutrality condition $n_i = n_e + Zn_{0d}$, where Z is normalized dust charge. In turn, Z was obtained from a force balance condition, which is the following: $m_d g + F_{id} = ZeE$, where m_d is dust particle mass, g is acceleration of gravity, E is discharge electric field, and F_{id} is ion drag force downward directed. According to various estimates [28,29], ion drag force varies from 10^{-13} to 3×10^{-13} N for our case. For calculations, we chose a value $F_{id} \approx 1.5 \times 10^{-13}$ N. Then we have $Z = (m_d g + F_{id})/eE \approx 8 \times 10^3$, and $n_i = 4.5 \times 10^{-8}$ cm $^{-3}$. In general, discharge parameters are regular for a glow

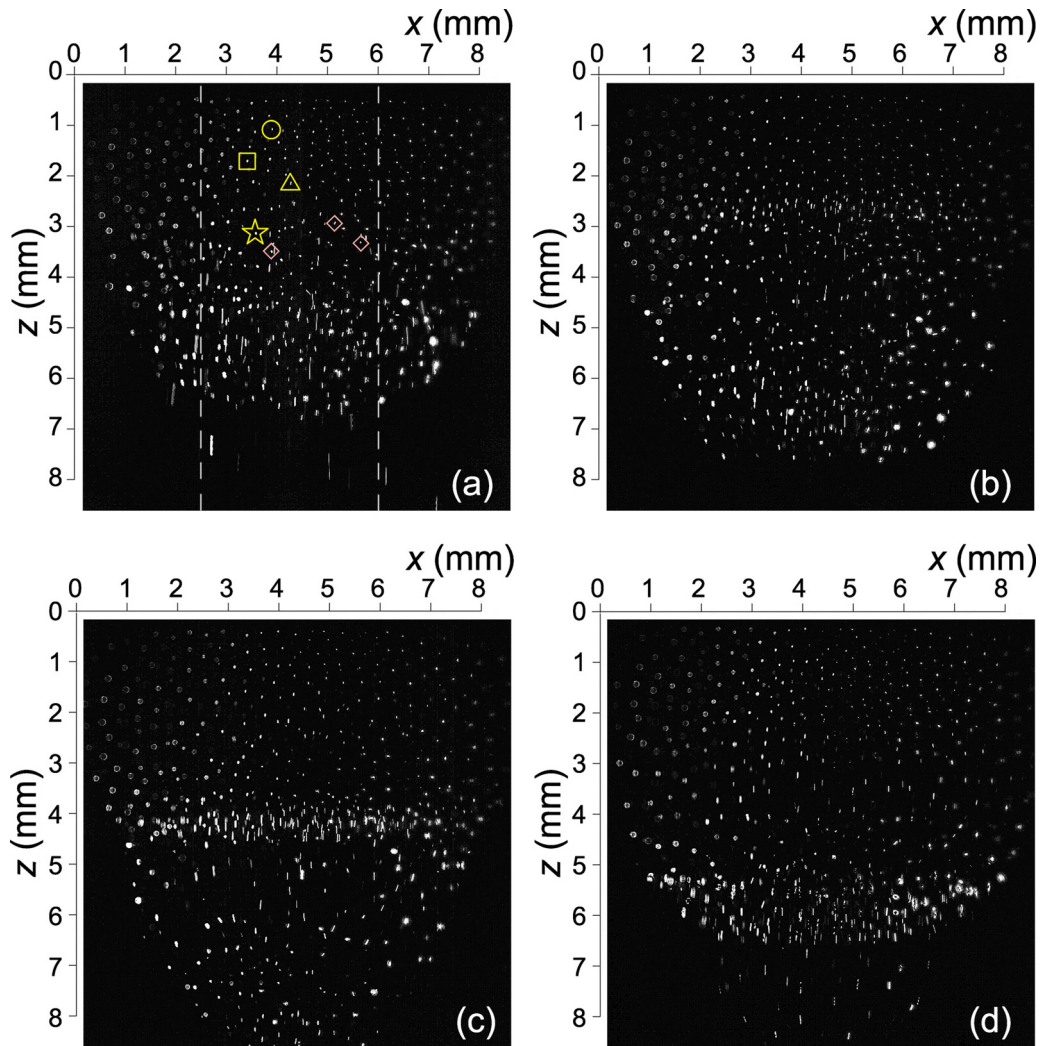


FIG. 2. Time evolution of dust-acoustic soliton: (a) $t = 0$, (b) $t = 26$ ms, (c) $t = 52$ ms, (d) $t = 78$ ms. (a) \circ corresponds to particle 1, \square to particle 2, \triangle to particle 3, \star to particle 4, and \diamond to particle group 5; vertical dashed lines denote analyzed area.

discharge [27,28]. Note that due to the presence of negatively charged dust particles, the ion concentration is several times higher than the electron concentration in accordance with the quasineutrality condition. Such a situation is common in dusty plasmas (see, for example [27,30]). The equations for calculating the Debye radius and dust-acoustic velocity are given in the next section.

At a pressure of 0.125 Torr the dust cloud had a clear, detectable crystalline structure, formed due to the action of the friction force, which reduces the kinetic energy of the particles. With a decrease in pressure (and therefore friction forces) a smooth transition to the liquid phase was observed. In this work we consider the waves in the liquid phase, although waves and oscillations of low frequency (~ 10 Hz) were observed throughout the entire range of pressures. The main reason for this choice is that the models describing such solitons are more general and suitable, within the accuracy of normalization, for the description of ion- and electron-acoustic solitons. Note that the study of dust-acoustic waves in the crystalline phase is also of interest [34], but is the subject of a separate study. Figure 2 shows the individual phases of the formation and breaking of the dust-acoustic solitary

wave. In our opinion, at the nonlinear stage of evolution the wave can be considered as a dust-acoustic soliton. The corresponding video is shown in the Supplemental Material [35]. We will discuss the classification of the observed wave in the Theoretical Model section. The considered process has been repeated with a period of ≈ 0.08 s.

In Fig. 2 it is clearly seen that the dust-acoustic wave, which is almost flat, forms in the upper part of the cloud, amplifies as it moves downward, and decays in the lower part of the dust cloud. Smoothed dust concentration profiles corresponding to Fig. 2 are shown in Fig. 3. The soliton velocity is $V_{\text{sol}} \sim 6$ cm/s, which agrees well with the dust-acoustic velocity value (Table I) taking into account supersonic nonlinear wave motion.

At first glance (Figs. 2 and 3), it may seem that it is a compression soliton, which is stationary most of the time. However, an analysis of the dynamics of dust particles has shown that the soliton has more sophisticated behavior during its lifetime, including its destruction and the occurrence of multistreaming flow.

From frame-by-frame analysis for particles marked in Fig. 2(a) we obtained their positions and vertical velocities,

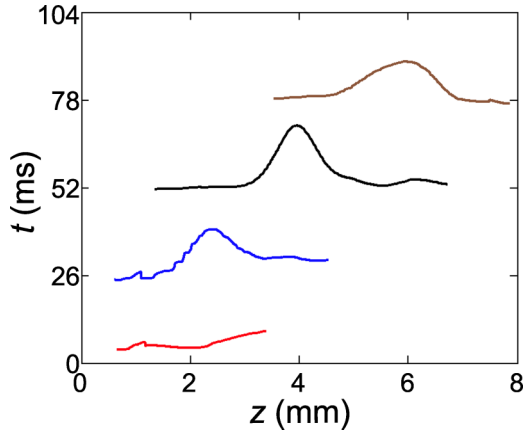


FIG. 3. Time evolution of dust concentration profiles, corresponding to Fig. 2.

which are plotted in Fig. 4. It should be noted that the dynamics of selected particles relates to the dynamics of most particles from the corresponding horizontal layer in the near-axial region $2.5 \text{ mm} < x < 6 \text{ mm}$ [as shown in Fig. 2(a) with dashed lines], where the wave can be considered flat.

The entire dust cloud can be divided into three areas in the vertical direction:

1. Soliton formation area within $0 \text{ mm} \leq z \leq 3 \text{ mm}$;

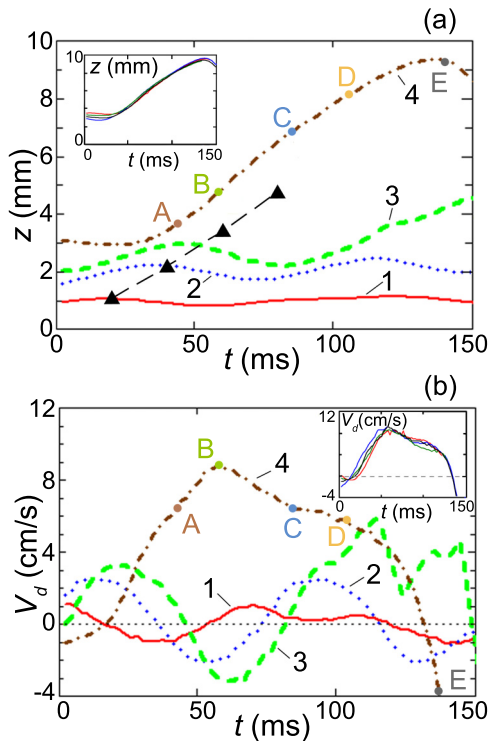


FIG. 4. Motion parameters of selected particles: (a) time dependency of z coordinate; (b) time dependency of particle longitudinal velocities. Subplots represent trajectories and velocities of other particles from the breaking region. These are particles of group 5, denoted by the \diamond symbols in Fig. 2(a).

2. Multistreaming flow formation area within $3 \text{ mm} \leq z \leq 4 \text{ mm}$;

3. Area of existence of soliton remnant within $4 \text{ mm} \leq z \leq 8 \text{ mm}$.

Let us consider these areas in detail.

1. As can be seen, at $z \leq 3 \text{ mm}$ the motion of particles is finite (particles 1, 2, 3) and has periodic nature. This stage of dust-acoustic instability was described in detail in [20,21]. In particular, it was shown that particle oscillations are due to resonance interaction with a self-excited dust-acoustic wave. The amplitude of the oscillations increases with increasing wave amplitude and nonlinearly steepening of the wave profile [21]. The maximum velocity of the oscillating particles tends to the phase velocity of the wave, and the dust concentration profile becomes steeper, reaching the minimum width and acquiring a solitonlike shape (bold curve in Fig. 1(c) from [21]). In [21], the Lagrangian-Eulerian model [36] was used to estimate the parameters of the wave process. In the framework of the soliton concept, the nonlinear stage of a similar phenomenon has been discussed in [24]. In particular, it was experimentally and theoretically shown in [24] that the particles move down in a single front under the influence of the soliton. The magnitude of their displacement is evaluated at units and tens of the Debye radii, λ_D . In this case, the upward movement, according to the authors, may be caused by external forces that tend to restore the undisturbed shape of the dust cloud. Among these are the gravity, electric force, friction, and ion drag forces. By the example of ion- and electron-acoustic solitons, it was shown in [22,23] that finite unidirectional movement of particles is an inherent property of solitons under consideration. In this case so-called “soliton currents” with unique properties are excited.

2. At $z \approx 3 \text{ mm}$ the soliton amplitude reaches a critical value, and the dust particles under the action of the soliton field acquire a velocity approximately equal to the velocity of the soliton (see Fig. 4, particle 4). Such particles are accelerated by the front of the soliton and move along with it to the lower edge of the dust cloud. Multistreaming flow develops, which in theory [12] reduces the wave energy. This process is called the breaking of a soliton [12] or a nonlinear wave [15,16,21]. In experiments on the study of a strong electron plasma wave [15], this phenomenon led to the generation of an accelerated electron flux, which was recorded with a gridded energy analyzer. The accelerated electrons gain approximately twice the wave phase velocity. In dusty plasma, particle acceleration can be observed directly. Dust particles accelerated by a breaking wave were also observed in [20] [see Figs. 4(a) and 4(b)] and in [21] [see tracks D, E, F, H in Fig. 3(a)]. Their speed was equal to the wave phase velocity. However, the process of generating accelerated particles as well as analysis of their properties was not the subject of a detailed study.

3. In our experiment, within the $4 \text{ mm} \leq z \leq 8 \text{ mm}$ region, the multistreaming flow converts the plasma in a turbulent state, which is observed in the lower part of the cloud below the breaking point (see the video in the Supplemental Material [35]). Particles accelerated by a soliton form a downward flow. The upward flow is formed by particles ejected from the cloud by the previous soliton. The action of external

forces tends to return them to their original unperturbed state. The motion of particles in the region below the breaking point ($z \geq 4$ mm) becomes very complicated; its analysis is beyond the scope of this article.

Let us further focus on the study of the soliton breaking process as well as particle acceleration in the breaking region. A breaking soliton is no longer a soliton from a mathematical point of view; however, as one can see from the experiment [see Figs. 2(c) and 2(d)], it can be quite stable reaching the lower boundary of the cloud without extreme broadening. It should be noted that in our experiment we did not observe any oscillations behind the soliton front, predicted in many collisionless models (see, for example, [12]).

After the breaking, trapped particles make a significant contribution to the wave concentration profile. This phenomenon is somewhat similar to ion capture by a dust-acoustic soliton [11], where the ion concentration profile consists of two types of ions—free and trapped. The difference is that dust-acoustic solitons are not a potential well for negatively charged particles. As will be shown below, the presence of trapped particles at the leading edge of the wave is explained by the action of the friction force. At the lower part of the cloud [Fig. 2(d)] the wave is scattered, and trapped particles are ejected outside the dust cloud.

Using traditional methods of dust-acoustic soliton studies based on the analysis of dust concentration profiles n_d it is impossible to detect soliton breaking. The position of the maximum of the function n_d at different times is marked in Fig. 4(a) with “▲” symbols. As mentioned above, the angle of inclination of the resulting straight line corresponds to the speed of the wave $V \approx 6$ cm/s, which can be approximately considered constant. Let us compare the speed of accelerated particles with the speed of the soliton. The trajectory of accelerated particles has a specific bend [the segment of curve 4 between points A and D in Fig. 4(a)]. The corresponding speed jump can be seen in Fig. 4(b) (the segment of curve 4 between points A and C). The maximum particle velocity is approximately one and a half times the wave velocity [point B in Fig. 4(b)]. The jump duration is $t_{V+} \approx 45$ ms, or $t_{V+}\omega_p \approx 14$ in the normalized form. Then, the particle velocity decreases to a speed approximately equal to the wave velocity [the segment between points C and D in Fig. 4(b)], and finally, it sharply reverses [the segment between points D and E in Fig. 4(b)]. The last segment corresponds to the return of ejected particles to the cloud under the action of external forces.

A theoretical interpretation of the results will be presented in the next section.

III. THEORETICAL MODEL

Soliton models are often used to describe the properties of self-excited solitary waves in space plasma [37–41]. In our experiment, in the dust cloud, only one wave crest is excited, which manages to go through all stages of evolution from self-excitation to breaking, accompanied by particle acceleration. Moreover, as can be seen from Figs. 2 and 3, the width of the wave concentration profile is much smaller than axial dimensions of the dust cloud, a profile shape is close to the soliton one, and the wave velocity exceeds the dust-acoustic

velocity by 1.8 times. Therefore, in our opinion, it is natural to describe the observed solitary wave (especially in a strongly nonlinear phase) within the framework of the soliton model. As mentioned above, the notion of “dissipative soliton” generalizes the notion of “classical soliton” for a nonconservative case [4,5]. It is important to note that the concept of dissipative solitons implies their self-excitation with a certain periodicity, which is observed in our experiment. The self-excited soliton is a convenient object to study breaking processes, as in this case there is a mechanism of amplifying of the soliton up to supercritical amplitude, which is absent in the case of induced excitation [42,43]. At the same time, weak dissipation has almost no effect on profiles, velocity, and other important properties of dust-acoustic solitons [7,8].

As shown in the previous section, the observed wave process is rather complex. In this paper we restrict ourselves to its qualitative description, which helps to explain important details. For a theoretical interpretation of the experimental results, we use a simple hydrodynamic model of dusty plasma without a magnetic field [44,45]. We assume that the plasma consists of electrons, singly charged ions, and “cold” negatively charged dust particles of constant radius. We write the system of normalized hydrodynamic equations in the form

$$N_e(\Phi) = \frac{n_e}{n_{e0}} = \exp\left(\frac{e\Phi}{T_e}\right) \equiv \exp\left(\frac{\Phi}{\beta\delta_i}\right), \quad (1)$$

$$N_i(\Phi) = \frac{n_i}{n_{i0}} = \exp\left(-\frac{e\Phi}{T_i}\right) \equiv \exp\left(-\frac{\Phi}{\delta_i}\right), \quad (2)$$

$$\frac{\partial N_d}{\partial t} + \frac{\partial N_d v_d}{\partial z} = 0, \quad (3)$$

$$\frac{\partial v_d}{\partial t} + v_d \frac{\partial v_d}{\partial z} = \frac{\partial \Phi}{\partial z}. \quad (4)$$

Here $\Phi = eZ\varphi/C_d^2 m_d$ is electrostatic potential; $C_d = \sqrt{Z^2 n_{d0} T_i / m_d n_{i0}}$ is dust-acoustic velocity; $\beta = T_e / T_i$. Concentrations, initial concentrations, and normalized concentrations of charged particles of the sort j are denoted, respectively: $n_j, n_{j0}, N_j = n_j / n_{j0}$, where $j = e, i, d$ for electrons, ions, and dust particles, respectively, $\delta_j = n_{j0} / Z n_{d0}$. Hydrodynamic dust particle velocity, v_d , is normalized to C_d . Variables z and t are normalized to λ_D and ω_d^{-1} , respectively, where $\lambda_D = \sqrt{T_i / 4\pi e^2 n_{i0}}$ is the Debye radius, and $\omega_d = \sqrt{4\pi Z^2 n_{d0} e^2 / m_d}$ the plasma frequency for dust component. In Eq. (4), only the action of the electric field of the soliton on charged particles is taken into account; the remaining forces are considered to be compensated. We do not use the model [8] here which takes into account the friction force for the following reasons. Firstly, the model [8] does not take into account the forces amplifying the soliton; therefore its amplitude decreases with time (in our case, the amplitude grows up to the breaking point). Secondly, for the case of weak dissipation, the soliton profiles in [8] are close to the classical $\propto \text{sech}^2(z)$ and can be obtained from the collisionless model, neglecting the evolution of the wave.

For the stationary case, we used a single variable $\xi = z - Mt$, where M is the Mach number equal to the ratio of the soliton velocity to C_d . Then from (3) and (4) one can get an

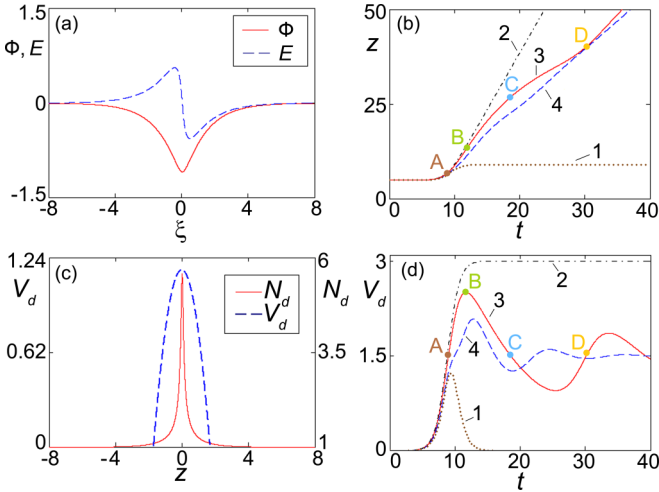


FIG. 5. Soliton parameters obtained from the numerical solution of Eqs. (6) and (8).

expression for N_d :

$$N_d(\Phi) = \frac{M}{\sqrt{M^2 + 2\Phi}}. \quad (5)$$

Now the problem can be reduced to a single Poisson equation:

$$\frac{d^2\Phi}{d\xi^2} = \delta_e N_e - \delta_i N_i + N_d. \quad (6)$$

Equation (6) allows single integration and analysis within the approach of the Sagdeev pseudopotential method [11]. In the mentioned paper [11] one can find a description of other methods of his analysis. We restrict ourselves here to simple numerical integration (6) by the Runge-Kutta method. The soliton solution at $\delta_i = 1.5$, $\beta = 60$, $M = 1.5$ is shown in Figs. 5(a) and 5(c). The potential profile $\Phi(\xi)$ is obtained from Eq. (6), and the profile of the electric field is obtained by the formula $E = -d\Phi/d\xi$. One can find the concentration profile $N_d(\xi)$ from (5).

The obtained solution is close to critical, since the soliton solution no longer exists at $M = 1.7$. The soliton width is $\Delta_\Phi = 3.2\lambda_D$, which is close to the experimentally obtained value. The hydrodynamic models do not allow one to calculate the parameters of the motion of individual particles; however, this can be done in the single-particle approximation developed for solitons in [22]. The motion equation for a dust particle can be written in the form

$$m_d \frac{d^2z}{dt^2} = Ze \frac{d\phi}{dz} - v_{dn} \frac{dz}{dt}, \quad (7)$$

where $v_{dn} = \frac{8\sqrt{2\pi}r_d^2 n_a T_a}{3m_d v_{Ta}}$ is the dust-neutral collision frequency (see, for example, [27] and references therein); $v_{Ta} = (T_a/m_a)^{1/2}$ is the thermal velocity of gas atoms. As the acting force we take into account

- (a) the electric force [first term on the right side of Eq. (7)], which is easy to calculate with a soliton solution [see Fig. 5(a)] of Eq. (6);

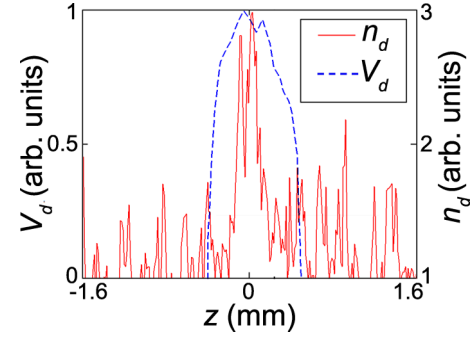


FIG. 6. Soliton profiles obtained from the analysis of experimental data at the horizontal level of $z \approx 3$ mm (see Fig. 2).

- (b) the friction force, which is described by the second term on the right side of Eq. (7).

Note that hereafter our theoretical model becomes non-self-consistent. Equation (7) with regard to the assigned normalization will take the form

$$\frac{d^2z}{dt^2} = \frac{d\Phi}{dz} - \Omega \frac{dz}{dt}, \quad (8)$$

where $\Omega = v_{dn}/\omega_d$. The value of Ω calculated on the basis of the data in Table I is $\Omega \approx 0.07 \ll 0.1$, which gives us the right to use the weak dissipation approximation. Analytical expressions for Φ can be obtained using the small amplitude approach. At this, Eq. (8) was solved for small amplitudes in [22] for ion-acoustic solitons. In our case, for solitons of arbitrary amplitudes, we use the numerically calculated dependence $\Phi(\xi) = \Phi(z - Mt)$ [see Fig. 5(a)]. Dependences $z(t)$ and $V_d(t) = dz/dt$ are shown in Figs. 5(b) and 5(d) for the plasma parameters given above and different values of Ω . Curve 1 corresponds to the motion of a dust particle in the field of the soliton with a subcritical amplitude, obtained earlier from Eq. (6). This case is in accord with the finite displacement of the dust particle at a distance $4\lambda_D$ in the direction of the soliton motion [see Fig. 5(b)]. The profile $V_d(t)$ displayed by curve 1 in Fig. 5(d) is solitonlike, symmetric with respect to the soliton center. The calculation results are in good agreement with [24].

In Fig. 5(c) the profiles of $V_d(z)$ and $N_d(z)$ are obtained from Eqs. (8) and (5), respectively. As can be seen, the velocity profile is several times wider than the concentration profile. Figure 6 shows the same not-smoothed profiles obtained experimentally. The results of the experiment and theory agree well.

An increase in the soliton amplitude to a supercritical value is the cause of its breaking [12]. The breaking leads to the appearance of multistreaming flow, and as a result, to the intersection of the trajectories of neighboring dust particles in the crest of the soliton. To simulate multistreaming flow, we increased the amplitude of the soliton by factor of 1.5, while its width and speed were considered to be constant for simplicity. The corresponding solutions of Eq. (8) are shown in Figs. 5(b) and 5(d), curves 2–4. As one can see, the case of $\Omega = 0$ [see Fig. 5(b), curve 2] differs from the cases $\Omega \neq 0$ (curves 3 and 4) by an angle of inclination of the obtained curves that is twice as large, and, consequently, a value of

V_d at $t \rightarrow \infty$ that is twice as large. Moreover, as follows from Fig. 5(d), at $t \rightarrow \infty$ the particle velocity is equal to the soliton velocity $V_d \approx M$ for $\Omega \neq 0$ (see curves 3 and 4), and it is twice the soliton velocity $V_d \approx 2M$ for $\Omega = 0$ (see curve 2). A dissipation-free solution is consistent with the results of [15] where the electrons were accelerated by a breaking electron plasma wave to speeds twice the phase velocity of a wave in a collisionless plasma (the corresponding experiment is described in [46]). Our experiment describes well the dissipative case $\Omega \neq 0$ [see Fig. 4(a), particle 4]. This hypothesis is also supported by the fact that when $\Omega \neq 0$, the accelerated particles experience oscillations, which follows from the numerical solution in Fig. 5(d), curves 3 and 4. The frequency and amplitude of oscillations depend on Ω , so their amplitude decreases, and the frequency increases with the growth of Ω . At the same time, a characteristic bend found earlier in the experiment appears on the trajectory graph [the sections between points A and D in Figs. 4(a) and 5(b), respectively].

At $\Omega = 0.1$, the maximum velocity which the particles attain during oscillations is one and a half times the phase velocity of the wave [point B in Fig. 5(d)], which also agrees well with experimental data [point B in Fig. 4(b)]. The particle velocity oscillation period after trapping is $T_V \approx 22$ [curve 3 in Fig. 5(d)]. On the experimental curves, only the first half period of oscillations is clearly detectable [the section between points A and C in Fig. 4(b)]. The “cutting off” of the oscillations is probably associated with the destruction (or transformation) of the soliton after the development of multistreaming, as well as with the boundedness of the dust cloud and plasma inhomogeneity, and other factors that are not taken into account in the theoretical model. However, the duration of the experimentally detected velocity jump ($t_{V+\omega_p} \approx 14$) is in reasonable agreement with the results of the theoretical model ($T_V/2 \approx 11$).

It should be noted that the velocities v_d and V_d are not identical; the first one describes the hydrodynamic velocity of the particle flux, and the second one describes the velocity of individual particles. The value of v_d can be expressed from Eq. (3) in the form [22] $v_d = M(1 - 1/N_d)$. It is easy to show that the v_d and V_d profiles are different, although their maximum values are equal. The presented soliton model is in good agreement with the model [21] because it consists of two parts, i.e., the hydrodynamic (Euler) one and the single-particle (Lagrange) approximation.

A breaking soliton loses energy due to particle acceleration. Therefore, in this case, there should be an energy pumping mechanism, which in our opinion is the ion flux. Detailed studies of ion drag and energy balance are the subject of subsequent work. In this paper, we restricted ourselves to only the study of wave evolution.

In conclusion, it is worth noting that the soliton stability after breaking has not been analyzed theoretically in detail, and we have only detected the evidence of the appearance of multistreaming flow. It is possible that a new wave structure may exist in a stationary mode.

As noted in [47,48], the friction force can be a stabilizing factor in evolving open systems. Indirectly, it is indicated by the fact that the trajectories of dust particles accelerated by the breaking of a soliton in the presence of friction forces have

the same asymptotics [see Fig. 5(b), curves 3 and 4], so due to dissipation, accelerated dust particles are localized at the front of the soliton, forming a single structure. In the absence of friction [see Fig. 5(b), curve 2]), accelerated particles quickly leave the neighborhood of the soliton. To answer the question about the stability of the soliton structure under study, we need more complicated theoretical models (see, for example, [8,11,49]) and experiments are required in a more extended dust cloud (see experiments in [50]). However, in any case, there will be an acceleration of charged dust particles up to speeds much higher than the average unperturbed velocity, which for particles in the upper part of the cloud is $\langle |V_d| \rangle \sim 0.1$ cm/s.

IV. CONCLUSIONS

The evolution of a plane dust-acoustic soliton in a dust cloud in glow discharge plasma is studied. Both macroscopic and kinetic parameters of the plasma near the soliton were experimentally determined. Namely, the macroscopic parameters are the dust concentration profiles and the speed of the wave, the kinetic one, is the individual dust particle's dynamic. The analysis of macroparameters did not allow us to detect the evidence of the soliton breaking. However, analysis of the trajectories of individual particles revealed the evolution of a soliton, including its breaking and the appearance of multistreaming flow. It was found that after reaching the critical amplitude the soliton front accelerates the particles to its own speed, which significantly (by several orders of magnitude) exceeds the average velocity of the particles in the unperturbed state. After the soliton breaks, the dust concentration profiles save their structure for some time. The velocity of motion of these profiles after breaking is also equal to the initial velocity of the soliton. Reaching the bottom edge of the dust cloud, the structure completely disintegrates, and accelerated particles are ejected far beyond the unperturbed cloud, causing plasma turbulence. The theoretical interpretation of the experimental results was performed using a simple hydrodynamic model, within which we obtained profiles of the electric field and potential, as well as the dust concentration profile. However, the hydrodynamic model is not relevant for the description of soliton breaking and the appearance of multistreaming flow, so we used a single-particle approach based on data obtained from the hydrodynamic theory to calculate the main parameters of the multistreaming flow. Thus, particle trajectories and velocity profiles of a breaking soliton were obtained. Both dissipative and nondissipative cases are considered. In the first case, the velocity of the accelerated particles and the velocity of the soliton are equal, and the particles experience damped oscillations when interacting with the wave, which reasonably agrees with the experimental results. In the nondissipative case, particles during the soliton breaking are accelerated to speeds twice as high compared with the wave speed, which can be important in analyzing turbulence and instabilities in collisionless plasma of tokomaks, space, etc. The soliton is supplied with energy, in our opinion, due to the ion drag.

The study of wave-particle interaction processes has become more active recently in the context of the search for new plasma methods of wave acceleration of charged particles

[25]. In this regard, dusty plasma is a convenient tool, since, as shown above, it makes it possible to study processes at the kinetic level using relatively simple methods.

ACKNOWLEDGMENT

This work was supported by the Russian Science Foundation, Grant No. 19-12-00354.

-
- [1] J. S. Russell, Report of the Committee on Waves, Report of the 7th Meeting of British Association for the Advancement of Science, Liverpool (John Murray, London, 1838), pp. 417–498.
- [2] E. Infeld and G. Rowlands, *Nonlinear Waves, Solitons, and Chaos* (Cambridge University Press, Cambridge, 2000).
- [3] C. S. Gardner, J. M. Greene, M. D. Kruskal, and R. M. Miura, *Phys. Rev. Lett.* **19**, 1095 (1967).
- [4] N. Akhmediev and A. Ankiewicz, *Dissipative Solitons, Lecture Notes in Physics Vol. 661* (Springer, Berlin, Heidelberg, 2005).
- [5] N. Akhmediev, A. Ankiewicz, J.-M. Soto-Crespo, and P. Grelu, *Int. J. Bifurcation Chaos* **19**, 2621 (2009).
- [6] I. S. Aranson and L. Kramer, *Rev. Mod. Phys.* **74**, 99 (2002).
- [7] S. Ghosh, A. Adak, and M. Khan, *Phys. Plasmas* **21**, 012303 (2014).
- [8] S. Khan, A. Rahman, F. Hadi, A. Zeb, and M. Z. Khan, *Contrib. Plasma Phys.* **57**, 223 (2017).
- [9] M. Q. Tran, *Phys. Scr.* **20**, 317 (1979).
- [10] M. Berthomier, R. Pottelette, M. Malingre, and Y. Khotyaintsev, *Phys. Plasmas* **7**, 2987 (2000).
- [11] P. K. Shukla and A. A. Mamun, *Introduction to Dusty Plasma Physics* (Institute of Physics Publishing, Bristol, UK, 2002).
- [12] *Reviews of Plasma Physics*, edited by R. Z. Sagdeev and M. A. Leontovich (Consultants Bureau Enterprises, Inc., New York, 1966), Vol. IV.
- [13] O. I. Bogoyavlenskii, *Russ. Math. Surv.* **45**, 1 (1990).
- [14] Y. Rattanachai and S. Phibanchon, *J. Phys.: Conf. Ser.* **1136**, 012009 (2018).
- [15] B. S. Bauer, A. Y. Wong, V. K. Decyk, and G. Rosenthal, *Phys. Rev. Lett.* **68**, 3706 (1992).
- [16] A. S. Sandhu, G. R. Kumar, S. Sengupta, A. Das, and P. K. Kaw, *Phys. Rev. Lett.* **95**, 025005 (2005).
- [17] J. M. Dawson, *Phys. Rev.* **113**, 383 (1959).
- [18] T. Katsouleas and W. B. Mori, *Phys. Rev. Lett.* **61**, 90 (1988).
- [19] B. S. Bauer, A. Y. Wong, L. Scurry, and V. K. Decyk, *Phys. Fluids B* **2**, 1941 (1990).
- [20] M. Schwabe, M. Rubin-Zuzic, S. Zhdanov, H. M. Thomas, and G. E. Morfill, *Phys. Rev. Lett.* **99**, 095002 (2007).
- [21] L.-W. Teng, M.-C. Chang, Y.-P. Tseng, and L. I., *Phys. Rev. Lett.* **103**, 245005 (2009).
- [22] F. M. Trukhachev and A. V. Tomov, *Cosmic Res.* **54**, 351 (2016).
- [23] F. M. Trukhachev, A. V. Tomov, M. M. Mogilevsky, and D. V. Chugunin, *Tech. Phys. Lett.* **44**, 494 (2018).
- [24] O. F. Petrov, F. M. Trukhachev, M. M. Vasiliev, and N. V. Gerasimenko, *JETP* **126**, 842 (2018).
- [25] E. Adli *et al.*, *Nature* **561**, 363 (2018).
- [26] N. N. Skvortsova, N. K. Kharchev, and K. A. Sarkisyan, *JETP Lett.* **70**, 201 (1999).
- [27] V. E. Fortov, A. G. Khrapak, S. A. Khrapak, V. I. Molotkov, A. P. Nefedov, O. F. Petrov, and V. M. Torchinsky, *Phys. Plasmas* **7**, 1374 (2000).
- [28] V. Yaroshenko, S. Ratynskaia, S. Khrapak, M. H. Thoma, M. Krestschmer, H. Höfner, and G. E. Morfill, *Phys. Plasmas* **12**, 093503 (2005).
- [29] S. A. Khrapak, A. V. Ivlev, G. E. Morfill, and H. M. Thomas, *Phys. Rev. E* **66**, 046414 (2002).
- [30] D. N. Polyakov, V. V. Shumova, L. M. Vasilyak, and V. E. Fortov, *Phys. Scr.* **82**, 055501 (2010).
- [31] S. A. Maiorov, *Bull. Lebedev Phys. Inst.* **39**, 51 (2012).
- [32] H. W. Ellis, R. Y. Pai, E. W. McDaniel, E. A. Mason, and L. A. Viehland, *At. Data Nucl. Data Tables* **17**, 177 (1976).
- [33] S. A. Maiorov, *Plasma Phys. Rep.* **35**, 802 (2009).
- [34] A. Homann, A. Melzer, S. Peters, R. Madani, and A. Piel, *Phys. Lett. A* **242**, 173 (1998).
- [35] See Supplemental Material at <http://link.aps.org/supplemental/10.1103/PhysRevE.100.063202> for a video fragment corresponding to Fig. 2, slowed down 100 times.
- [36] C.-T. Liao, L.-W. Teng, C.-Y. Tsai, C.-W. Io, and Lin I, *Phys. Rev. Lett.* **100**, 185004 (2008).
- [37] R. V. Reddy and G. S. Lakhina, *Planet. Space Sci.* **39**, 1343 (1991).
- [38] H. Matsumoto, H. Kojima, T. Miyatake, Y. Omura, M. Okada, I. Nagano, and M. Tsutsui, *Geophys. Res. Lett.* **21**, 2915 (1994).
- [39] S. Bounds, R. F. Pfaff, S. F. Knowlton, F. S. Mozer, M. A. Temerin, and C. A. Kletzing, *J. Geophys. Res.* **104**, 28709 (1999).
- [40] R. Trines, R. Bingham, M. W. Dunlop, A. Vaivads, J. A. Davies, J. T. Mendonça, L. O. Silva, and P. K. Shukla, *Phys. Rev. Lett.* **99**, 205006 (2007).
- [41] J. Shi, M. N. S. Qureshi, K. Torkar, M. Dunlop, Zh. Liu, and T. L. Zhang, *Ann. Geophys.* **26**, 1431 (2008).
- [42] D. Samsonov, A. V. Ivlev, R. A. Quinn, and G. Morfill, and S. Zhdanov, *Phys. Rev. Lett.* **88**, 095004 (2002).
- [43] P. Bandyopadhyay, G. Prasad, A. Sen, and P. K. Kaw, *Phys. Rev. Lett.* **101**, 065006 (2008).
- [44] N. N. Rao, P. K. Shukla, and M. Y. Yu, *Planet. Space Sci.* **38**, 543 (1990).
- [45] N. Ya. Kotsarenko, S. V. Koshevaya, G. A. Stewart, and D. Maravilla, *Planet. Space Sci.* **46**, 429 (1998).
- [46] T. Tanikawa, A. Y. Wong, and D. L. Eggleston, *Phys. Fluids* **27**, 1416 (1984).
- [47] I. Prigogine and I. Stengers, *Order Out of Chaos* (Bantam Books, Toronto, 1984).
- [48] Yu. L. Klimontovich, *Phys.-Usp.* **39**, 1169 (1996).
- [49] F. M. Trukhachev, O. F. Petrov, M. M. Vasiliev, and E. Yu. Sevryugov, *J. Phys. A: Math. Theor.* **52**, 345501 (2019).
- [50] M.-C. Chang, L.-W. Teng, and Lin I, *Phys. Rev. E* **85**, 046410 (2012).